Vibrational dynamics of the WOW and WOOW bridge bonds: polarized infrared and Raman spectra of monoclinic $KBi(WO_4)_2$ single crystal

1994 J. Phys.: Condens. Matter 6 10263

(http://iopscience.iop.org/0953-8984/6/47/009)

J. Phys.: Condens. Matter 6 (1994) 10263–10271. Printed in the UK

Vibrational dynamics of the W–O–W and W(–O)(–O)–W bridge bonds: polarized infrared and Raman spectra of monoclinic $KBi(WO_4)_2$ single crystal

J Hanuza†, M Maczka† and J H van der Maas‡

† W Trzebiatowski Institute for Low Temperature and Structure Research, Polish Academy of Sciences, Wroclaw, Poland

‡ University of Utrecht, Faculty of Chemistry, The Netherlands

Received 12 April 1994, in final form 25 July 1994

Abstract. Polarized Raman spectra in the 40–1000 cm^{-1} frequency range and polarized reflection IR spectra in the 580–1000 cm^{-1} range were measured for the $KBi(WO_4)_2$ single crystal. Factor group analysis has been performed and the results of these calculations were used to determine the nature of the observed phonons. The spectra obtained are interpreted on the basis of the dimer structure plus weak perturbations corresponding to W–O···W interactions.

1. Introduction

In the last years a few papers have been published relating to the luminescence properties of a large variety of inorganic phosphors such as Nd^{3+}-, Am^{3+}-, Np^{3+}-, Pu^{3+}- and Ce^{3+}-doped $NaBi(WO_4)_2$ [1–3]. Our aim is to study the luminescence and electronic properties of Cr^{3+}-doped $KBi(WO_4)_2$ (member of the alkali-metal bismuth tungstates family). As understanding of the vibrational and electron level distribution is the basis for the explanation of the laser properties, this work deals with examination of IR and Raman spectra of potassium–bismuth double tungstate. The electron–phonon coupling plays a crucial role in the energy transfer between the active ions. The vibronic patterns of the emission spectra often contain lines corresponding to the crystal matrix. Therefore the phonon properties of $KBi(WO_4)_2$ play an important role in determining the use of this material as the host crystal for Cr^{3+} dopant ions.

2. Experimental details

The crystals have been grown by the thermal method developed by Borisov and Klevtsova [4] and Klevtsov *et al* [5].

The single crystals were oriented using the x-ray method. Polarized IR reflection spectra were measured with a Perkin–Elmer FTIR stereo zoom 7 microscope connected with a Perkin–Elmer 2000 FTIR spectrometer, by averaging 128 scans for each spectrum. The spectra were measured with the incident angle close to 0°. The numerical aperture of the

0953-8984/94/4710263+09$19.50

Cassegrain objective and condenser is 0.60, permanently aligned. The sample stage working distance is 24 mm and the measurements were performed with an aperture diameter of 600 μm. A mercury cadmium telluride detector was used, and spectra were recorded with a resolution of 4 cm^{-1}. Using standard IR DM software, calculations were carried out on a PC to transform reflection spectra into transmission spectra. The program used transforms specular reflectance spectra into absorbance spectra by the Kramers–Kronig integration method. A method formulated by the group of Jones [6] of the National Research Council of Canada was employed in the calculation of the integration.

The low-temperature spectra of the $KBi(WO_4)_2$ in a KBr pellet were recorded at a resolution of 2 cm^{-1} on a Mattson 5020 spectrometer using an RIIC-VLT-2 variable-temperature unit equipped with KBr windows and connected to a West M2071 microprocessor-based controller. Liquid nitrogen was used as coolant. Second-derivative spectra were calculated on a PC using the standard Mattson First™ software.

Raman spectra were recorded in back-scattering geometry using a Perkin–Elmer 1760X FTIR spectrometer, equipped with a Raman module. As an excitation source the 1064 nm line of a YAG:Nd^{3+} laser and $In_xGa_{1-x}As$ detector operating at liquid-nitrogen temperature was used. All spectra were recorded at 2 cm^{-1} resolution, and the laser output power was 300 mW. The $In_xGa_{1-x}As$ detector enabled us to record spectra only to 200 cm^{-1}. The spectra in the region 40–300 cm^{-1} were measured with a cooled GaAs Burle photomultiplier connected to a double DFS 24 spectrometer. The excitation source was the 488 nm line of an argon laser (output power, 150 mW; resolution, 2 cm^{-1}).

3. Crystal structure and selection rules

The $KBi(WO_4)_2$ crystallizes in the monoclinic space group $C_{2h}^6(C2/c)$ with four molecules per unit cell. Its crystal parameters are $a = 8.25$ Å, $b = 10.60$ Å, $c = 7.62$ Å and $\beta = 93.8°$ [7]. This double tungstate is isostructural with the α-$KY(WO_4)_2$ phase for which $a = 8.05$ Å, $b = 10.35$ Å, $c = 7.54$ Å and $\beta = 94°$ [8]. In later studies this structure was described using a new set of basic vectors: $a_1 = a + c$, $b_1 = b$ and $c_1 = c$. Relevant lattice parameters are $a_1 = 10.64$ Å, $b_1 = 10.35$ Å, $c_1 = 7.54$ Å and $\beta = 130.5°$ [4,5]. The unit-cell projection of this crystal on the a–c plane is presented in figure 1.

The structure of this tungstate family is formed of W_2O_8 dimers which are coupled to each other through the W⟨O⟩W oxygen bridges, forming $(W_2O_8)_n$ ribbon. The eight-coordinated Bi polyhedra and twelve-coordinated K polyhedra are bounded by the edges forming the cationic layer.

The unit cell of this tungstate contains four formula units. However, since it contains two non-equivalent $KBi(WO_4)_2$ groups, the primitive cell with two formula units was selected as a basis for the factor group analysis (FGA). This analysis was performed by assuming that the structure consists of dimers and that interactions between the dimers leads to some weak perturbations. Table 1 summarizes the FGA predictions. According to these calculations a total of 72 ($K = 0$) unit-cell modes are distributed between $\Gamma_T = A_u + 2B_u$ acoustic modes, $\Gamma_{T'} = 2A_g + 4B_g + 4A_u + 5B_u$ translational modes, $\Gamma_L = 3A_g + 3B_g$ librational modes and $\Gamma_N = 12A_g + 12B_g + 12A_u + 12B_u$ internal modes. In this work, IR spectra were recorded parallel and perpendicular to the b axis. Since $b \| y$ appears in the $E \| b$ polarization only, A_u modes are active in this arrangement. In $E \perp b$ polarization, only B_u modes are IR active because the transition vectors of the B_u modes lie within the a–c plane and are not symmetry fixed. To determine A_g modes the Raman spectrum was recorded with both

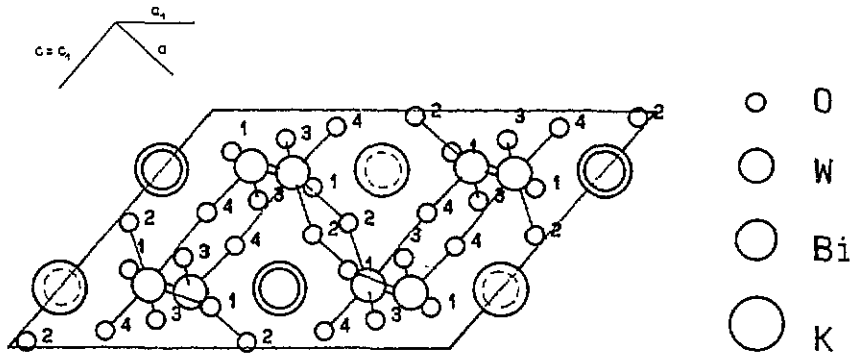

Figure 1. The structure of the $KBi(WO_4)_2$ unit cell projected on the a–c plane. The numbers describe the set of non-equivalent oxygen atoms.

incident and scattered light polarized parallel to the b axis, i.e. $c(bb)\bar{c}$. For B_g modes the Raman spectrum was measured with incident light polarized parallel to the b axis and scattered light polarized perpendicular to the b axis.

Table 1. Factor group analysis for $KBi(WO_4)_2$ crystal ($C2/c$; $Z = 4$).

					Unit-cell modes					Activity	
C_{2h}	E	$C_2(b)$	i	σ_h	n(N)	n(T)	n(T′)	n(L)	n(int)	IR	Raman
A_g	1	1	1	1	17	0	2	3	12	—	XX, YY, ZZ, XZ
B_g	1	−1	1	−1	19	0	4	3	12	—	XY, YZ
A_u	1	1	−1	−1	17	1	4	0	12	Y	—
B_u	1	−1	−1	1	19	2	5	0	12	X, Z	—
					72	3	15	6	48		
$U_R(p)$	24	4	0	0	↑	↑	↑	↑			
$U_R(s)$	6	4	2	0	↑	↑	↑	↑			
$U_R(s-v)$	2	0	2	0	↑	↑	↑	↑			
$\chi_\rho(R)_N$	72	−4	0	0	→↑	↑	↑	↑			
$\chi_\rho(R)_T$	3	−1	−3	1	—	→↑	↑	↑			
$\chi_\rho(R)_{T'}$	15	−3	−3	−1	—	—	→↑	↑			
$\chi_\rho(R)_L$	6	0	6	0	—	—	—	→↑			

4. Results and discussion

The energy gap in the 450–700 cm^{-1} region is characteristic of crystals where oxyions form isolated tetrahedra, as in scheelite crystals [9–15]. Since the tungstate anions in $KBi(WO_4)_2$ form a polymeric structure, even in this region several lines are observed. These lines correspond to the oxygen bridge bond vibrations connected with the existence of 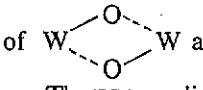 systems in this structure.

The FGA predicts that 48 internal modes are divided into $5A_g+5B_g+5A_u+5B_u$ stretching

species and $7A_g + 7B_g + 7A_u + 7B_u$ bending species. All the tungsten and oxygen atoms are on sites of C_1 symmetry. However, for the W_2O_{10} cluster resulting from the W_2O_8 dimer plus weak W⋯O⋯W perturbations the site symmetry is C_i. The method of ascent in symmetry predicts in this case for the stretching region four W⋯O⋯W bridge modes, four W⋯O⋯W bridge modes and four terminal W–O modes per dimer. Since there are two dimers in the primitive unit cell, there should be 24 stretching modes and therefore the number of stretching vibrations should increase to six for each crystal spectrum.

The energy of stretching vibrations falls in the 500–1000 cm^{-1} region, where bands have the strongest intensities for both IR and Raman spectra. In general, the observed spectra are similar to those obtained for other crystals of the same structure. Each Raman spectrum (see figure 2(*a*) for $c(bb)\bar{c}$ polarization and figure 2(*c*) for $a(bc)\bar{a}$ polarization and table 2) consists of five singlets and one triplet. In the case of $KLn(WO_4)_2$ (Ln≡Sm–Lu or Y), each Raman spectrum also consists of six bands but each of them splits into two or three components [16, 17]. The bands at 870, 776, 756 and 519 cm^{-1} are shifted by 7–35 cm^{-1} towards lower frequencies and those at 709–693 and 637 cm^{-1} by 10–20 cm^{-1} towards higher frequencies in comparison with similar bands for $KLn(WO_4)_2$. By comparing relative intensities of all lines for A_g and B_g spectra, one can see that two strongest bands at 870 and 756 cm^{-1} are highly polarized. They are symmetric modes of the terminal and W⋯O⋯W bridge bond systems, respectively. The line at 776 cm^{-1} can be assigned to the asymmetric stretching vibration of the terminal bond. The remaining lines at 637 and 519 cm^{-1} originate from the W⋯O⋯W bridge vibrations, and triplet 693–709 cm^{-1} from the W⋯O⋯W double-bridge vibrations.

The polarized IR spectra (see figure 3(*a*) for $\boldsymbol{E}\|\boldsymbol{c}$ and figure 3(*b*) for $\boldsymbol{E}\|\boldsymbol{b}$ and table 2) consist in this region of six bands and are consistent with the FGA predictions based on a polymeric structure of the tunsten–oxygen cluster. The centres of gravity of these bands are at 918, 898, 870–858, 824–789, 749–747 and 599 cm^{-1}. These bands are shifted towards lower frequencies by 10–30 cm^{-1} in comparison with similar bands in $KLn(WO_4)_2$. The A_u spectrum differs from the B_u spectrum by different shifts of bands and their intensities. These shifts are only 2 and 3 cm^{-1} for the lines at about 749 and 901 cm^{-1} but are quite large for the lines at 870 cm^{-1} (about 12 cm^{-1}) and 812 cm^{-1} (about 23 cm^{-1}). Such large shifts may result from technical reasons as the reflection technique may lead to some slight distortion of the spectra due to imperfection of the reflection plane of the crystal studied. The changes in relative intensities for A_u and B_u spectra are very large. The IR absorption intensities of the light polarized in the direction of *b* and *c* axes are proportional to the squares of the components of DM change on these axes. The proportionality factors calculated for stretching vibrations taken for molecular orientations presented in figure 1 are given in table 3. From this table we see that the stretching modes of W⋯O⋯W single-bridge system (W–O(4) and W–O(4′) bonds) should show most of their intensities in the light polarized parallel to the *c* axis. Therefore very strong and broad band at 580–600 cm^{-1} should be assigned to W⋯O⋯W vibration. The bands at about 790–810 and

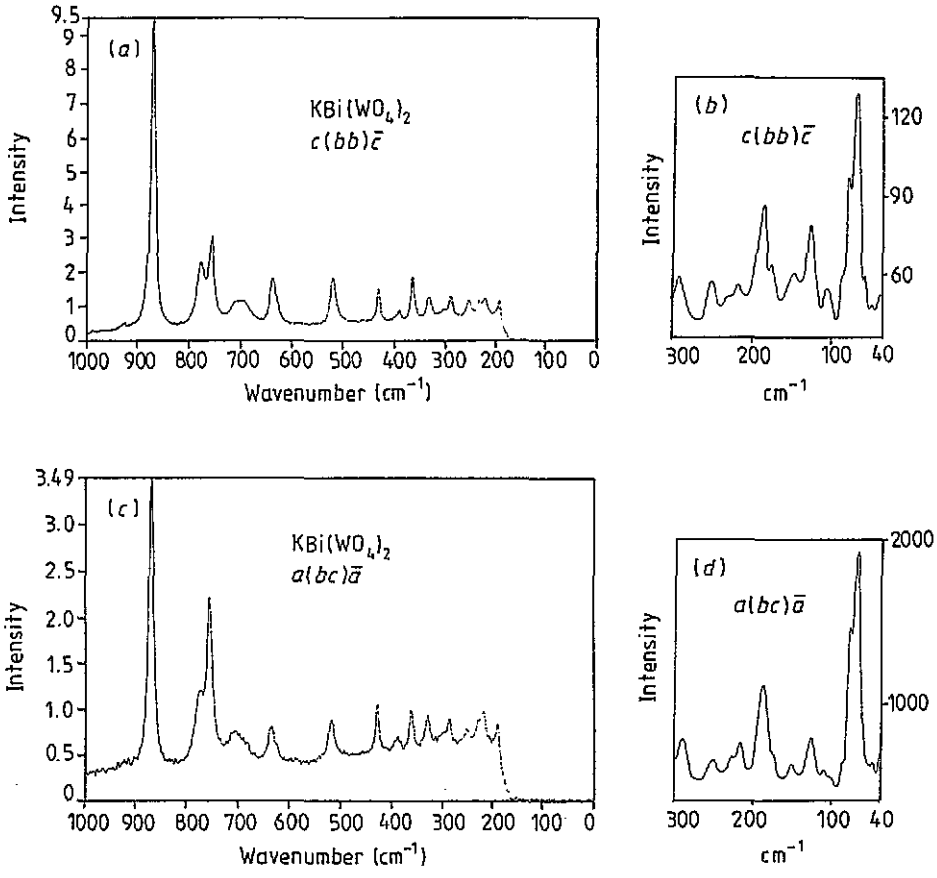

Figure 2. Polarized Raman spectra for a $KBi(WO_4)_2$ single crystal.

740 cm^{-1} are much more intense in the A_u spectrum (light polarized along the *b* axis) than in the B_u spectrum (light polarized along the *c* axis). By inspection of table 3, one can see that such behaviour should be expected both for W–O(2), W–O(2′) bonds corresponding to the 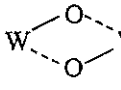 bridge system and W–O(1), W–O(3) terminal bonds. By analogy to our former studies of $KLn(WO_4)_2$ [16, 17] we assigned these bands to the 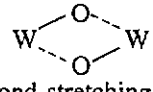 double-bridge vibrations. The remaining bands can be ascribed to terminal bond-stretching vibrations.

The temperature dependence spectra show no phase transition in the 120–295 K temperature range. Both 295 and 120 K spectra reveal six bands in the range 950–700 cm^{-1} (table 4). In the room-temperature spectrum these bands are at 917, 867, 822, 802, 748 and 719 cm^{-1}. The low-temperature spectrum reveals the same bands and only bands at 748 and 822 cm^{-1} are shifted by 3 and 2 cm^{-1} towards higher frequencies. Moreover, all bands are broader at room-temperature spectrum owing to anharmonicity.

Table 2. Polarized IR and Raman spectra for $KBi(WO_4)_2$ single crystal.

IR spectra		Raman spectra		
A_u modes $\| b$	B_u modes $\| c$	A_g modes $c(bb)\bar{c}$	B_g modes $a(bc)\bar{a}$	Assignments
918m		924vw		
901w	898s			
870w	858s	870vs	871vs	$\nu(WO_n)$ stretching modes
824sh	789m			
812s		776m	774m	
		756m	757s	
		709w	708w	
749m	747sh	700w	700sh	ν(W 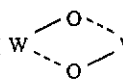 W) stretching modes
		694w	693sh	
			684sh	
599s	~580vs	637w	637w	
			629sh	ν(WOW) stretching modes
		519w	519w	
		431w	430w	
		398sh		
		390vw	384w	δ(OWO) bending modes
		365w	365w	
		333w	332w	
		304vw	300sh	
		289w	288w	δ(WOW) bending modes
		253w	252w	
		231w	230w	
		219w	219w	T'(K^+)
		189m	189m	
		177w	177sh	
		150w	154w	
		129w	129w	T'(Bi^{3+}) and T'(W^{6+})
		106w	111w	
			104w	
		86sh	87sh	
		78w	79w	L(WO_6)
		71s	71s	
		58w		
		50vw	50w	optic–acoustic coupled modes

5. Internal bending vibrations

As was shown above, 12 of 30 vibrational modes of the W_2O_{10} cluster are stretching vibrations and the remaining 18 modes are the bending modes. Therefore the number of crystal bending modes should increase to nine for each symmetry. However, the degeneracy of vibrations in the dimeric structure is expected to reduce the number of bending modes. This is in agreement with experiment. In the bending-mode region there are seven or eight bands, depending on polarization (see figures 2(*a*) and 2(*b*) for the $c(bb)\bar{c}$ polarization and figures 2(*c*) and 2(*d*) for the $a(bc)\bar{a}$ polarization). All these bands are shifted in comparison with corresponding bands of potassium lanthanide double tungstates $KLn(WO_4)_2$ to lower frequencies by 3–30 cm^{-1}. The energy range of bending vibrations extends from 430 to

Table 3. Proportionality factors for the intensity of the IR bands corresponding to W–O stretching vibrations.

	Squares of the components on the following axes		
Bond	*a* axis	*b* axis	*c* axis
W–O(1)	0.6452	0.2164	0.1014
W–O(2)	0.4892	0.3355	0.2038
W–O(2′)	0.7062	0.2728	0.00004
W–O(3)	0.1531	0.7898	0.0697
W–O(4)	0.0008	0.1930	0.8335
W–O(4′)	0.0164	0.1026	0.8501

Table 4. Temperature shifts of the IR bands for a $KBi(WO_4)_2$ crystal studied at 295 and 120 K: m, medium, s, strong; sh, shoulder.

IR band (cm^{-1})		$\Delta\nu$
295 K	120 K	(cm^{-1})
917m	917m	0
867m	867m	0
822sh	824sh	2
802s	802s	0
748s	751s	3
719sh	719sh	0

250 cm^{-1} and is very broad in comparison with simple tungstates for which it does not exceed 130 cm^{-1}. Such a large energy level splitting is characteristic for compounds with a polymeric structure. Comparison of the Raman spectra reveals that the lines at 430 and 332 cm^{-1} are much more intense in the B_g spectrum than in the A_g spectrum. The same behaviour was also observed for double tungstates $KLn(WO_4)_2$. The bands in the range 250–333 cm^{-1} are assigned to W–O–W and 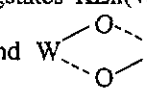 bridge vibrations by analogy to other oxygen bridge systems [18].

6. External modes

Below 250 cm^{-1} we expect to observe the external modes attributed to translational and rotational motions of the unit-cell components.

Studies of $CaWO_4$ [9–12] showed that translational modes of the Ca^{2+} ion, which has almost the same atomic weight as K^+, are observed in the range 196–275 cm^{-1}. We noticed in our previous studies of $KLn(WO_4)_2$ [16, 17] that T' (K^+) are observed in the range 230–260 cm^{-1}. These observations enable us to describe the bands at 177–231 cm^{-1} as translational modes of K^+ ions. Numerous studies of simple tungstates MWO_4, where M ≡ Ca, Sr, Ba or Pb, showed that the translational modes are approximately proportional to the square root of the appropriate reciprocal reduced masses [9–13]. This is in good agreement with our studies. The translational modes of Bi^{3+} ions (atomic mass, 209) are observed for $KBi(WO_4)_2$ at 104–154 cm^{-1} (see figure 2(*b*) for the $c(bb)\bar{c}$ polarization and figure 2(*d*) for the $a(bc)\bar{a}$ polarization). This is also in agreement with the observations made by Akimov *et al* [10] who observed the frequency of the translational mode for

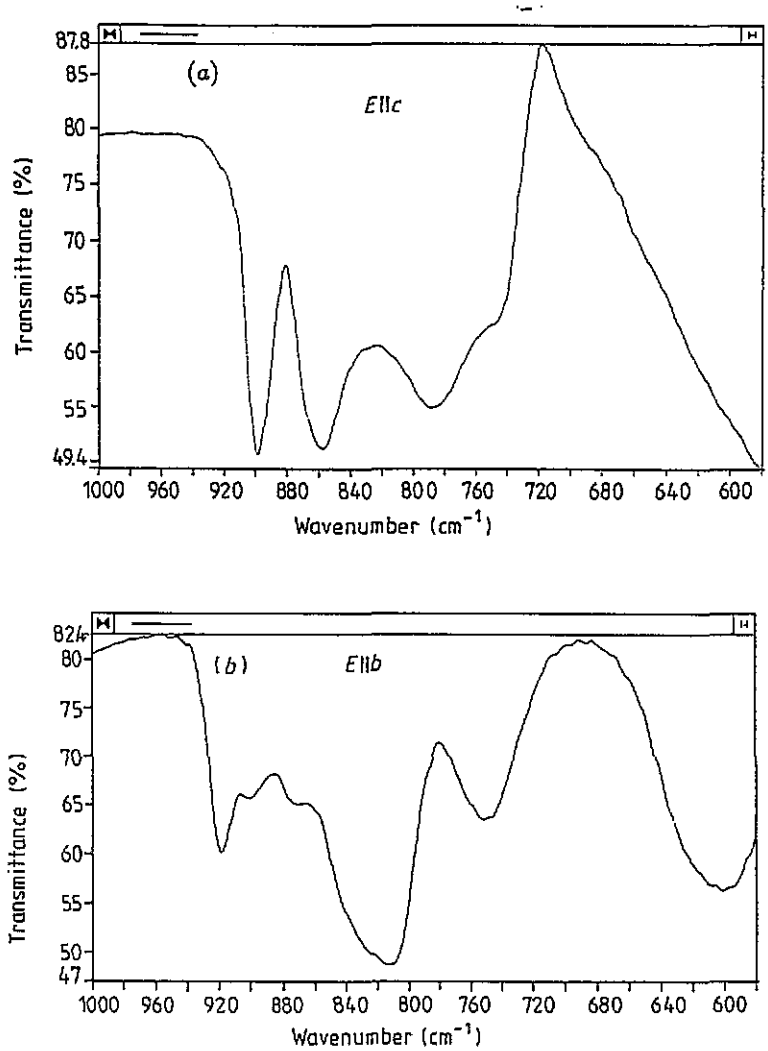

Figure 3. Polarized IR spectra for a $KBi(WO_4)_2$ single crystal.

Pb^{2+} ion (atomic mass, 207; close to that of Bi^{3+}) at 126 cm^{-1}. In the same region also the translational modes of WO_4^{2-} are expected. The librational vibrations are observed for simple tungstates in the range 195–290 cm^{-1} [9–11, 13–15]. Our previous studies of polymeric tungstates [16, 17] demonstrated, however, that, for the compounds in which polymeric oxalate system is formed, the librational modes could be decreased to 70 cm^{-1}. In the present study these modes are observed in the range 71–87 cm^{-1} (see figures 2(*b*) and 2(*d*)). Our assignment is further supported by comparison of the relative intensities of the observed lines. The bands at about 71–80 cm^{-1} are much more intnse than those at 100–230 cm^{-1}. Having in mind that the librational vibration leads to a large change in polarizability we should assign the most intense bands to the librational modes. The bands at 50 and 58 cm^{-1} can be assigned as optic–acoustic coupled modes.

7. Conclusion

When the polarized IR and Raman spectra are taken into account, it was demonstrated that the structure of $KBi(WO_4)_2$ consists of the hexacoordinated WO_6 polyhedra connected by the W–O–W and 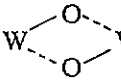 bridge bonds. As a result of this structure a very large splitting (about 400 cm^{-1}) for internal stretching vibrations of the WO_6 system is observed. We found that internal stretching modes fall into the region 510–924 cm^{-1}, and bending modes in 250–430 cm^{-1}; the external modes are observed below 250 cm^{-1}. The number of observed modes is larger than the FGA predicts. In the internal-modes region, one should expect 12 vibrations for both the A_g and the B_g spectrum while in our present study we observe 17 bands. This is mainly because the FGA does not take into account the weak interactions between W_2O_8 dimers, leading to formation of 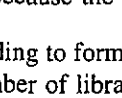 single-bridge bonds. In the external-modes region the number of librational modes is in good agreement with that predicted by the FGA. The number of observed translational modes is larger than predicted, probably because of strong coupling between these modes and internal bending modes.

The $KBi(WO_4)_2$ compound does not exhibit any phase transition in the range from 120 to 300 K. The stability of potassium–bismuth double tungstate is very important in view of possible application of this compound as the host lattice for Cr^{3+} ions. During melting, $KBi(WO_4)_2$ decomposes [7] but it is very stable in humid environments. This compound seems to be highly prospective host material for use in the production of $MBi_{1-x}Cr_x(WO_4)_2$ quantum generators.

Acknowledgment

This work was supported by the Polish State Committee for Scientific Research under grant 2 P303 069 06.

References

[1] Kaminski A A, Kholov A, Klevtsov P V and Khafizof S Kh 1989 *Neorg. Mater.* **25** 1054
[2] Gliva V R, Novikov Yu P and Myasoedov B F 1989 *J. Radioanal. Nucl. Chem. Lett.* **135** 307
[3] Nitsch K, Nikl M, Barta C, Schultze D, Triska A and Vecker R 1990 *Phys. Status Solidi* (a) **118** K133
[4] Borisov S V and Klevtsova R F 1968 *Kristallografiya* **13** 517
[5] Klevtsov P V, Kozeeva L P and Khartzenko L Yu 1975 *Kristallografiya* **20** 1210
[6] Hawranek J P, Neelakantan P, Young R C and Jones R N 1976 *Spectrochim. Acta* A **32** 86
[7] Klevtsov P V, Vinokurov V A and Klevtsova R F 1973 *Kristallografiya* **18** 1192
[8] Klevtsov P V, Kozeeva L P and Klevtsova R F 1968 *Neorg. Mater.* **4** 1147
[9] Akimov A N, Nikanovitsch M V, Ksenofontova N M and Umreiko D S 1985 *Zh. Prikl. Spektrosk.* **42** 621
[10] Akimov A N, Nikanovitsch M V, Popov B G and Umreiko D S 1986 *Zh. Prikl. Spektrosk.* **45** 225
[11] Nicol M and Durana J F 1971 J. Chem. Phys. **54** 1436
[12] Tarte P and Ligeois-Duyckaerts M 1972 *Spectrochim. Acta* A **28** 2029, 2037
[13] Khanna R K and Lippincott E R 1968 *Spectrochim. Acta* A **24** 905
[14] Barker A S 1964 *Phys. Rev.* **135** A 742
[15] Russel J P and Loudon R 1965 *Proc. Phys. Soc.* **85** 1029
[16] Hanuza J and Macalik L 1987 *Spectrochim. Acta* A **43** 361
[17] Hanuza J 1986 *Acta Phys. Pol.* A **70** 585
[18] Jezowska-Trzebiatowska B and Hanuza J 1973 *J. Mol. Struct.* **19** 109, and references therein